

Both human ferredoxins equally efficiently rescue ferredoxin deficiency in *Trypanosoma brucei*

Piya Changmai,^{1,2} Eva Horáková,¹ Shaojun Long,^{1†}
Eva Černotíková-Stříbrná,¹ Lindsay M. McDonald,^{1‡}
Esteban J. Bontempi^{1§} and Julius Lukeš^{1,2*}

¹Institute of Parasitology, Biology Centre and ²Faculty of Science, University of South Bohemia, Branišovská 31, 37005 České Budějovice (Budweis), Czech Republic.

Summary

Ferredoxins are highly conserved proteins that function universally as electron transporters. They not only require Fe-S clusters for their own activity, but are also involved in Fe-S formation itself. We identified two homologues of ferredoxin in the genome of the parasitic protist *Trypanosoma brucei* and named them *TbFdxA* and *TbFdxB*. *TbFdxA* protein, which is homologous to other eukaryotic mitochondrial ferredoxins, is essential in both the procyclic (= insect-transmitted) and bloodstream (mammalian) stage, but is more abundant in the active mitochondrion of the former stage. Depletion of *TbFdxA* caused disruption of Fe-S cluster biogenesis and lowered the level of intracellular haem. However, *TbFdxB*, which is present exclusively within kinetoplastid flagellates, was non-essential for the procyclic stage, and double knock-down with *TbFdxA* showed this was not due to functional redundancy between the two homologues. Heterologous expressions of human orthologues *HsFdx1* and *HsFdx2* fully rescued the growth and Fe-S-dependent enzymatic activities of *TbFdxA* knock-down. In both cases, the genuine human import signals allowed efficient import into the *T. brucei* mitochondrion. Given the huge evolutionary distance between trypanosomes and humans, ferredoxins clearly have ancestral and highly conserved function in eukaryotes and both human orthologues have

retained the capacity to participate in Fe-S cluster assembly.

Introduction

Iron-sulphur (Fe-S) clusters are ancient cofactors found in every domain of life. They can function as electron donors and/or acceptors, sulphur donors and sensors for specific molecular conditions and in a typical cell are likely to serve numerous other, as yet unknown functions (Lill, 2009). In eukaryotic cells, well over a hundred proteins requiring Fe-S clusters for their function have been identified so far, of which mitochondrial respiratory complexes I through III, ferredoxin, aconitase and DNA repair enzymes are among the best known (Rouault, 2012). Although well studied for decades, the eukaryotic DNA polymerases I through IV were only very recently shown to contain Fe-S clusters (Netz *et al.*, 2012). Hence, it is reasonable to anticipate that the importance of Fe-S cofactors is still underestimated.

In the yeast *Saccharomyces cerevisiae*, in which it has been studied extensively, the Fe-S cluster (ISC) assembly takes place in mitochondria with the participation of at least a dozen proteins. Core participants include the cysteine desulphurase complex (Nfs-Isd11), which provides sulphur to the scaffold protein IscU (Zheng *et al.*, 1993; Adam *et al.*, 2006; Wiedemann *et al.*, 2006; Shi *et al.*, 2009) and frataxin, generally considered to be an iron donor, although direct evidence for this function is still lacking (Stemmler *et al.*, 2010). In addition to these core proteins, ferredoxin and its reductase provide electrons, while a number of other proteins including Isa1/2 and Iba57 perform more specialized functions (Lange *et al.*, 2000; Li *et al.*, 2001; Mühlhoff *et al.*, 2007; Long *et al.*, 2011).

A number of distinct systems exist for the biogenesis of Fe-S clusters: the sulphur assimilation (SUF) machinery of prokaryotes and a handful of eukaryotes; the bacterial and mitochondrial ISC system, the prokaryotic nitrogen-fixing (NIF) machinery and, finally, the eukaryotic cytosolic (CIA) pathway (Py and Barras, 2010; Tsoulos *et al.*, 2012). With the exception of the SUF pathway, all of these machineries contain a system for electron transfer (Lill,

Accepted 13 May, 2013. *For correspondence. E-mail jula@paru.cas.cz; Tel. (+420) 387775416; Fax (+420) 385310388. Present addresses: [†]Institute for Cell and Molecular Biosciences, Faculty of Medical Science, Newcastle University, Newcastle, UK; [‡]Institute of Immunology & Infection Research, University of Edinburgh, Edinburgh, UK; [§]Instituto Nacional de Parasitología 'Dr. M. Fatala Chabén', Ministerio de Salud, Buenos Aires, Argentina.

2009). The ISC machinery acquires NADH-derived electrons via the ferredoxin and ferredoxin-reductase complex for the reduction of cysteine-bound S⁰ to the Fe-S cluster component S²⁻ (Kakuta *et al.*, 2001; Mühlenhoff *et al.*, 2003). *In vitro* experiments revealed that in the bacterium *Azotobacter vinelandii* ferredoxin also acts as a reductant in the formation of a single [4Fe-4S]²⁺ cluster from two [2Fe-2S]²⁺ clusters on the homodimeric IscU scaffold (Chandramouli *et al.*, 2007).

Saccharomyces cerevisiae contains only one homologue of ferredoxin (Yah1), while there are two homologues in humans, namely ferredoxins 1 (HsFdx1) and 2 (HsFdx2) (Shi *et al.*, 2012). Surprisingly, although HsFdx1 and Yah1 belong to type II ferredoxins, which contain the Pro-His motif while HsFdx2 belongs to type I ferredoxins (Seeber, 2002), only HsFdx2 is able to complement Yah1-depleted yeast cells (Sheftel *et al.*, 2010). Both HsFdx1 and HsFdx2 are expressed ubiquitously, with the former being highly expressed in the adrenal cortex and medulla, while the latter is abundant in the central nervous system (Sheftel *et al.*, 2010; Shi *et al.*, 2012). Investigation of the relevance of each homologue to Fe-S cluster assembly has produced conflicting results. While Sheftel *et al.* (2010) found only HsFdx2 to be involved in this process, Shi *et al.* (2012) determined both homologues to be necessary. Numerous other important roles have been identified for ferredoxins. Using electrons from NADPH-dependent ferredoxin reductase, HsFdx1 also participates in mammalian steroid hormone biosynthesis as a reductant of mitochondrial cytochrome P450 enzymes (Ewen *et al.*, 2011). In yeast, Yah1 together with Arh1 and Cox15p have a role in hydroxylation of haem *o* to haem *a* (Barros *et al.*, 2001) and coenzyme Q biosynthesis (Pierrel *et al.*, 2010). Hence, the depletion of Yah1 leads to defects in ISC assembly, haem synthesis and iron homeostasis (Lange *et al.*, 2000; Sheftel *et al.*, 2010; Miao *et al.*, 2011; Shi *et al.*, 2012).

In this study we identified two homologues of ferredoxin in the genome of the parasitic protist *Trypanosoma brucei*, a causative agent of highly pathogenic African sleeping sickness of humans and other diseases of animals. During their life cycle, trypanosomes alternate between the procyclic stage (PC), with a fully active reticulated mitochondrion, and the bloodstream stage (BS), for which an organelle highly reduced in morphology and function is characteristic (Besteiro *et al.*, 2002; Lukeš *et al.*, 2005). Since this excavate model flagellate is amenable to various methods of reverse genetics, we undertook functional analysis of both ferredoxins, termed here *TbFdxA* and *TbFdxB*. These analyses revealed that *TbFdxA* but not *TbFdxB* is essential for PC *T. brucei*, where it participates in Fe-S biogenesis. This feature makes trypanosomes suitable for heterologous functional analysis of human

ferredoxins. Interestingly, *TbFdxA* knock-down was efficiently rescued by both human orthologues, which restored the viability of the cells and their ability to form Fe-S clusters.

Results

Identification and phylogenetic analysis of ferredoxins in T. brucei

A BLAST search using the Yah1 sequence of *S. cerevisiae* as a query produced two significant hits within the genome of *T. brucei*. The corresponding small proteins, which we call *TbFdxA* (Tb927.7.890) and *TbFdxB* (Tb927.4.4980), have calculated molecular weights 19.71 kDa and 17.62 kDa respectively. Both *TbFdxA* and *TbFdxB* were predicted to have mitochondrial localization by MitoProtII, with 0.9829 and 0.8525 probabilities, respectively, and with similarly high probabilities predicted by pSORT.

At the protein level, *TbFdxA* and *TbFdxB* respectively share 39% and 33% identity with the yeast orthologue Yah1, while the identity between the two trypanosome proteins is 40%. Both *TbFdxA* and *TbFdxB* contain a conserved fer2 superfamily domain with a 2Fe-2S binding domain and a catalytic loop that may participate in catalysing electron transfer in redox reactions (Marchler-Bauer *et al.*, 2011). Conserved homologues of both proteins containing cysteine residues proposed to be responsible for the ligation of Fe or Fe-S clusters and other conserved motifs (Fig. 1A), were also found in the genomes of related kinetoplastid flagellates, including *Trypanosoma cruzi*, *Leishmania major*, *Leishmania braziliensis* and *Leishmania infantum* (Fig. S1A).

In order to reveal the phylogenetic position of the *T. brucei* ferredoxins within eukaryotes, we constructed a maximum likelihood phylogenetic tree (Fig. 1B). Unexpectedly, *TbFdxA* and *TbFdxB* are not closely related to one another. Neither is specifically related to any of the major eukaryotic groups. Although the clade containing *TbFdxA* is more closely related to the human and yeast ferredoxins than *TbFdxB* (Fig. 1B), its position is rather unstable and dependent on the taxon sampling (Fig. S1B). On the other hand, our analyses consistently reveal that *TbFdxB* belongs to the basal-most eukaryotic ferredoxin clade known so far. Interestingly, this clade contains a single trypanosomatid paralogue, whereas four *Leishmania* paralogues are present. Although the branching support was rather weak, the topology shown in Fig. 1B hints at the presence of at least one additional trypanosomatid paralogue that was lost during evolution. It also suggests the existence of a specific selective pressure that retains multiple paralogues present in the transcriptome of *Leishmania* spp.

A

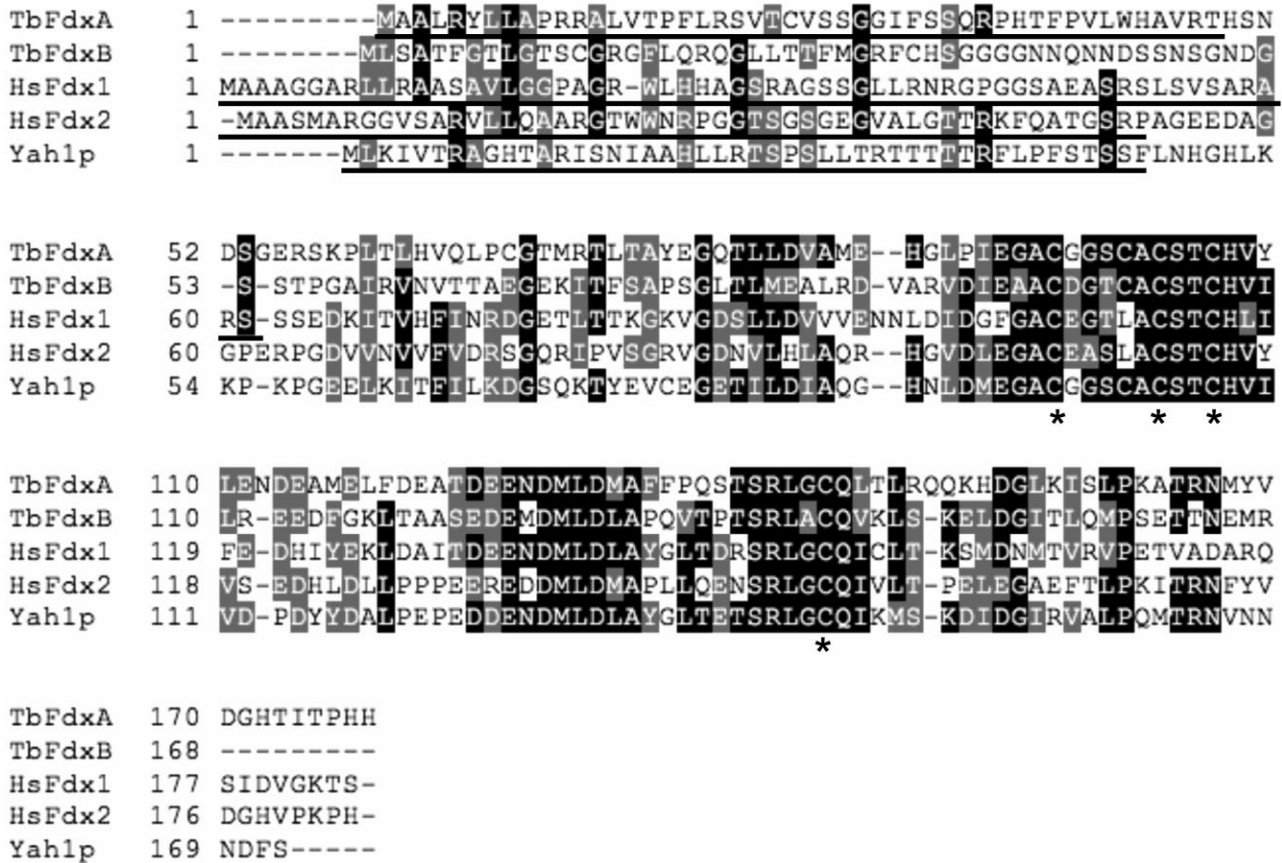


Fig. 1. Phylogenetic analysis of *TbFdxA* and *TbFdxB*.

A. Multiple sequence alignment of ferredoxins in *T. brucei*, *H. sapiens* and *S. cerevisiae*. The alignment was generated using CLUSTALW (<http://www.ch.embnet.org/software/ClustalW.html>) and Boxshade (http://www.ch.embnet.org/software/BOX_form.html). Identical residues are highlighted in black and conserved residues in grey. Conserved cysteine residues of the Fe-S motif are marked with asterisks. Underlines represent predicted mitochondrial targeting sequences by MitoProtII.

B. Maximum likelihood phylogenetic analysis of ferredoxins inferred using RAxML and Γ -corrected LG matrix (LG+ Γ model). Branching support is expressed via non-parametric bootstrap support and Bayesian posterior probabilities. See *Experimental procedures* for details.

Localization of ferredoxins in *T. brucei*

Although both ferredoxins (*TbFdxA* and *TbFdxB*) were predicted to have mitochondrial localization with similarly high probabilities, we tested their localization experimentally. Having specific polyclonal antibody only against *TbFdxA* (see below), we decided to fused both proteins on their C-terminus with V5 tag. The resulting tetracyclin (Tet)-inducible constructs *TbFdxA*_pT7_V5 and *TbFdxB*_pT7_V5 were electroporated into wild-type PC and clonal cell lines were selected using puromycin. Two clones from each cell line were examined 2 days after the addition of Tet using indirect immunofluorescence. As shown in Fig. 2A, both ferredoxins fully colocalized with Mitotracker Red, confirming their mitochondrial localization.

TbFdxA is essential for cell growth of the procyclic stage

To establish protein expression and depletion levels of the *TbFdxA* and *TbFdxB* proteins, we expressed both full-size His₆-tagged proteins in *Escherichia coli*, from which the abundantly expressed insoluble brown proteins were purified. Specific polyclonal antibodies generated in rats against the expressed *TbFdxA* and *TbFdxB* proteins did immunodecorate *TbFdxA*, but failed to recognize the latter protein (data not shown). Therefore, we compared the abundance of only *TbFdxA* in individual life stages. As shown in Fig. 2B, the protein is highly expressed in the PC trypanosomes, but is much less abundant in the BS cells.

In order to assess the function of individual ferredoxins in PC, we used RNAi to selectively deplete the mRNA

B

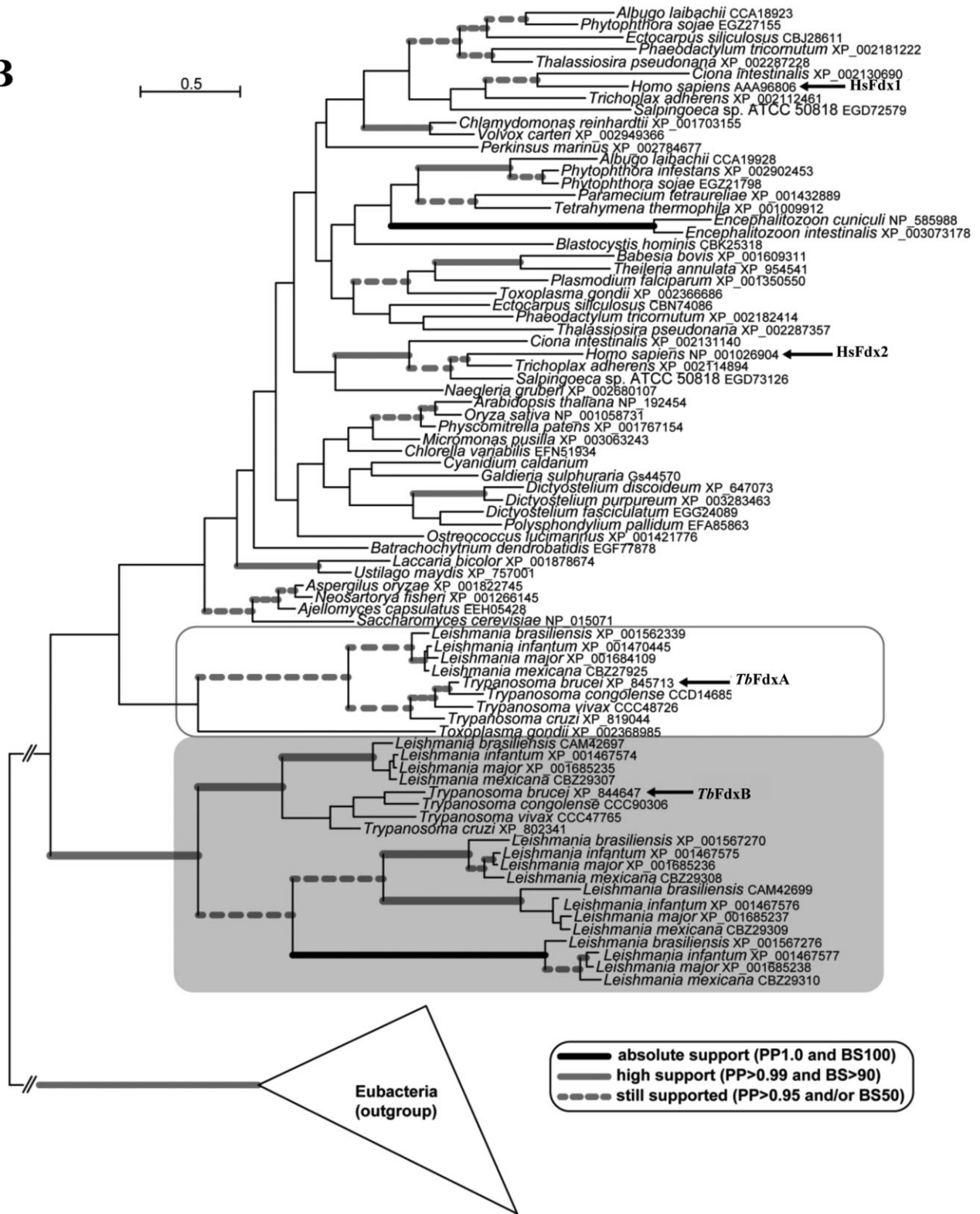


Fig. 1. cont.

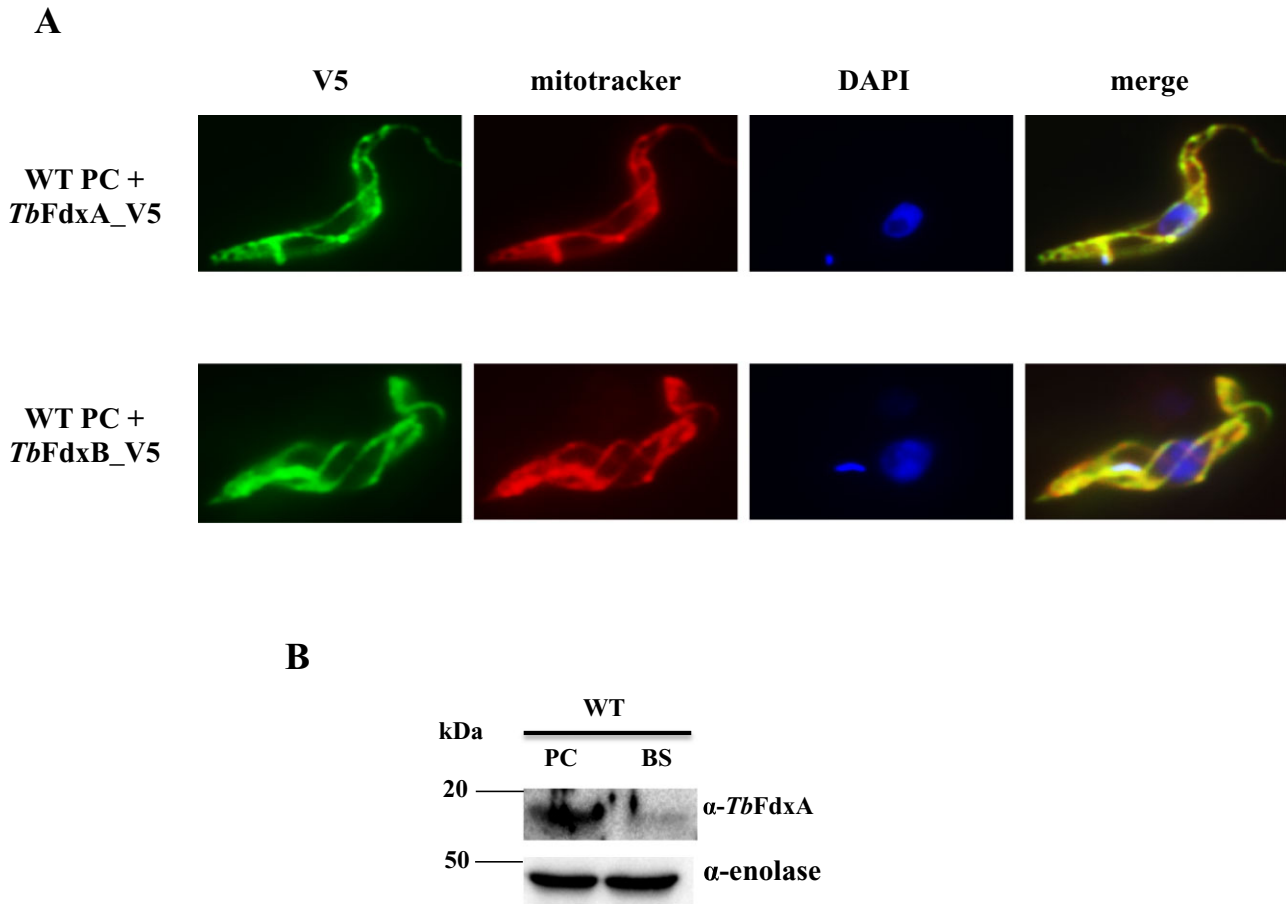


Fig. 2. *TbFdxA* and *TbFdxB* localize to the mitochondrion of *T. brucei*.

A. Fluorescence microscopy of the wild-type PC cell line expressing *TbFdxA_V5* or *TbFdxB_V5* fusion protein. Mitotracker Red staining visualizes the mitochondrion. 4,6-diamidino-2-phenylindole (DAPI) stains nuclear and mitochondrial DNA.

B. Western analysis of protein level of *TbFdxA* in the wild-type PC and BS.

levels of *TbFdxA* and/or *TbFdxB*. Fragments of both genes were cloned into the p2T7-177 vector containing opposing Tet-regulatable promoters. Another construct was also generated with fragments of the *TbFdxA* and *TbFdxB* genes cloned in tandem to allow their parallel ablation. Parental *T. brucei* 29-13 cells were transfected with the NotI-linearized p2T7-177 constructs, and clonal cell lines were obtained by limiting dilution using phleomycin as a selectable marker.

RNAi induction impacted the studied cell lines differently: single *TbFdxA* and double *TbFdxA+B* knock-downs showed significantly reduced proliferation (Fig. 3A and C), whereas the growth of the *TbFdxB* RNAi cell line was not affected at all (Fig. 3B). The depletion of the target proteins was monitored by Western blot analysis using α -*TbFdxA* antibodies and in the case of *TbFdxB* by quantitative real-time PCR (Fig. 3). In the *TbFdxA* and *TbFdxA+B* RNAi cell lines where *TbFdxA* mRNA was targeted, a total elimination of the *TbFdxA* protein occurred (Fig. 3A and C). The target mRNA was also efficiently

depleted in the single *TbFdxB* knock-down as well as in the double knock-down (Fig. 3D). Western blot analysis also showed that the depletion of *TbFdxA* had no effect on the levels of other component of the ISC pathway namely Nfs, IscU and frataxin (Fig. S2). These results demonstrate that *TbFdxA*, but not *TbFdxB*, is essential for the viability of PC *T. brucei*.

TbFdxA is indispensable for the bloodstream stage

The BS of *T. brucei* harbours a mitochondrion which is substantially reduced in terms of morphology and metabolism, lacking the respiratory chain, fumarase and other activities (Tielens and van Hellemond, 1998; Besteiro *et al.*, 2005; Lukeš *et al.*, 2005; Coustou *et al.*, 2006). Consequently this stage relies on glycolysis for its fast growth. While the mitochondrial Fe-S cluster-containing proteins may therefore theoretically be bypassed in this life stage, this is not the case for numerous cytosolic and nuclear proteins requiring clusters for their activities.

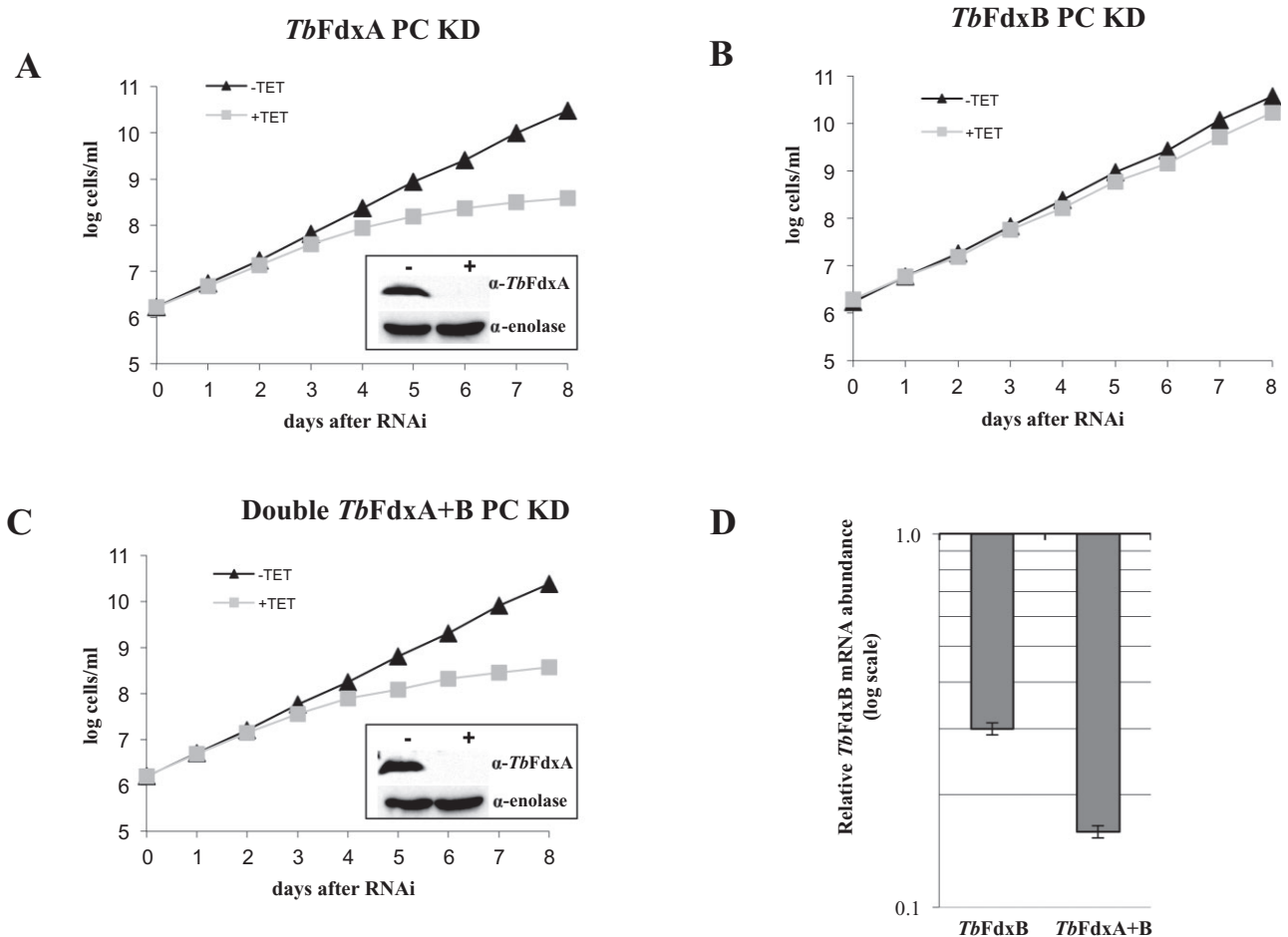


Fig. 3. *TbFdxA* but not *TbFdxB* is essential for growth of PC *T. brucei*.

A–C. Growth curves represent numbers of non-induced (triangles; black line) and RNAi-induced (squares; grey line) cell lines for single *TbFdxA* (A), single *TbFdxB* (B) and double *TbFdxA+B* knock-down PC cells (C). The y-axis represents the log scale product of cell density and total dilution. The data show a single representative experiment of biological triplicates. *TbFdxA* protein levels were analysed by Western blot analysis with α -*TbFdxA* antibody in whole-cell lysates from non-induced (–) and RNAi-induced (+) single *TbFdxA* (A) and double *TbFdxA+B* knock-downs (C) after 5 days of induction. Enolase was used as a loading control.

D. Quantitative real-time PCR analysis of *TbFdxB* mRNA was performed on cDNAs generated from the non-induced and RNAi-induced single *TbFdxB* and double *TbFdxA+B* knock-down cells 5 days after RNAi induction. The relative change in *TbFdxB* mRNA abundance upon tetracycline addition was determined by using 18S rRNA as internal reference. The means and SD values of three independent experiments are shown.

Indeed, Fe-S cluster-containing DNA polymerase and RNase L inhibitor (RLI), highly conserved proteins required for genomic DNA replication and cytosolic translation respectively, are clearly essential for both *T. brucei* stages (Estévez *et al.*, 2004; Bruhn *et al.*, 2011). Comparative Western blot analysis of the PC and BS cells revealed that the level of *TbFdxA* protein in the latter stage is less than 17% of that in the insect dwelling stage (Fig. 2B).

We further investigate the role of *TbFdxA* in the BS, using the same RNAi strategy as for the PC. Surprisingly, we did not observe any growth defect in this knock-down even if the level of *TbFdxA* protein dropped by 96% as shown by Western analysis (Fig. S3). This result did not allow us to adequately distinguish as to whether *TbFdxA* was insuffi-

ciently depleted to cause a growth phenotype, or whether this protein is non-essential for the BS cells. Therefore, we resorted to a knockout strategy via homologous recombination (Fig. 4A and B), which leads to the disruption of both alleles of a single-copy gene, such as *TbFdxA*, resulting in total elimination of the corresponding protein. The presence of a regulatable copy of *TbFdxA* allows us to conclusively address whether the protein is indispensable for the BS of *T. brucei*. A previously described knockout strategy (Schnauffer *et al.*, 2001) was followed by replacing one allele of *TbFdxA* with a hygromycin-resistance cassette. Next, a plasmid allowing ectopic expression of the *TbFdxA* protein under the control of a Tet-responsive element was introduced into the single knockouts (1KO). This allows

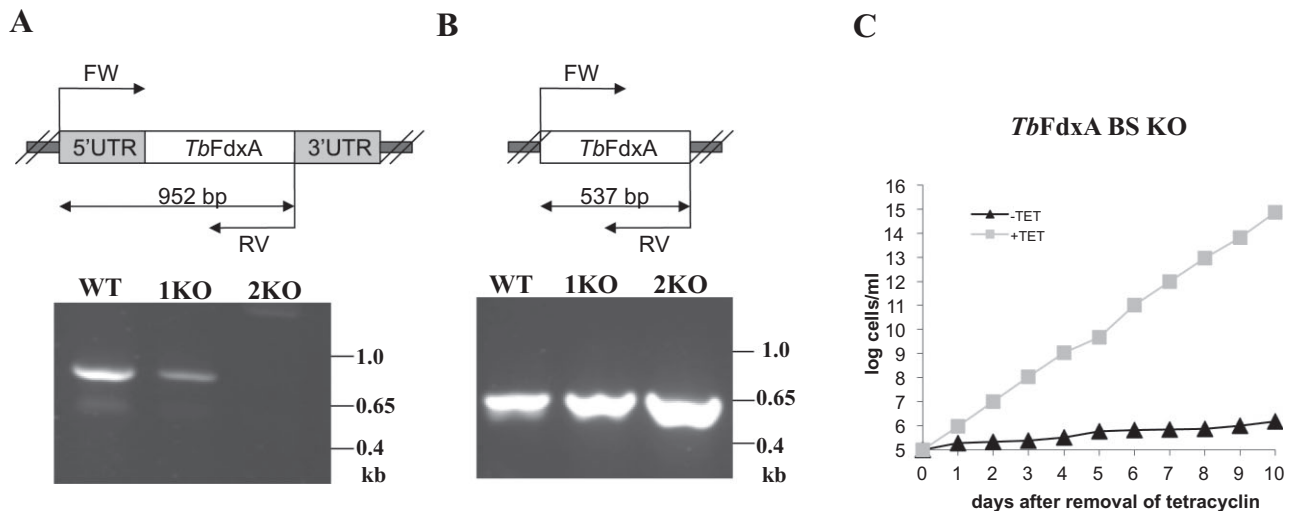


Fig. 4. *TbFdxA* is indispensable for viability of BS *T. brucei*.

A and B. PCR showing the absence of the endogenous *TbFdxA* gene in *TbFdxA* knockout cell line (A) and presence of the ectopic copy of *TbFdxA* (B). DNA was isolated from wild-type (WT), single allele replacement (1KO) and second allele replacement (2KO) BS cell lines. C. Growth curve represents numbers of *TbFdxA* knockout cell line grown in the presence (squares; grey line) or absence of tetracycline (triangles; black line). The data show a single representative experiment of biological triplicates.

proliferation of cells in the presence of Tet even when an essential gene is lost. Indeed, even when the second *TbFdxA* allele was subsequently disrupted by a neomycin-resistance cassette (2KO), the BS cells remained alive while the medium was supplemented with Tet. However, they immediately and completely lost viability when the drug was withdrawn (Fig. 4C), strongly indicating that the expression of an ectopic *TbFdxA* is vital for the survival of these flagellates. Elimination of the endogenous *TbFdxA* was confirmed using specific forward and reverse primers, annealing to the 5'UTR and part of the *TbFdxA* ORF, resulting in a 952-bp-long amplicon (Fig. 4A), confirmed by sequencing. Presence of the ectopic copy was verified by PCR with specific primers for full-length *TbFdxA* producing a 537 bp amplicon (Fig. 4B). All in all, the results obtained from the conditional knockout confirmed the essentiality of *TbFdxA* for the BS cells, although this stage seems to contain a far lower amount of the protein relative to PC (Fig. 2B). Consequently, despite the presence of only a rudimentary mitochondrion in the mammalian stage, the obtained results are compatible with active Fe-S cluster assembly in the organelle.

TbFdxA is required for synthesis of cytosolic and mitochondrial Fe-S proteins

Early studies suggested that the yeast and human ferredoxins are involved in mitochondrial *de novo* Fe-S cluster assembly, most likely functioning as electron donors (Lange *et al.*, 2000). We examined the effect of depletion of both ferredoxins on selected cytosolic and mitochondrial Fe-S enzymes in the PC trypanosomes.

In *T. brucei*, about 70% and 30% of aconitase, which is encoded by a single gene, is distributed in the cytosol and mitochondrion respectively (Saas *et al.*, 2000). This feature allows us to monitor its activity separately in both compartments (Fig. 5). The purity of each cell compartment, obtained by digitonin fractionation, was controlled by Western blot using antibodies specific for mitochondrial Hsp70 and cytosolic enolase (Fig. S4). As shown in Fig. 5A and C, both cytosolic and mitochondrial aconitase dropped by about 70% upon triggering RNAi of *TbFdxA* and *TbFdxA+B*. However, no decrease was observed in cytosolic and mitochondrial aconitase activities upon ablation of *TbFdxB* (Fig. 5B). The activity of succinate dehydrogenase (complex II), a Fe-S cluster-containing enzyme that is confined to the mitochondrion, followed the pattern observed for aconitase (Fig. 5D), whereas the reduction in activity of another Fe-S enzyme, cytochrome *c* reductase (complex III), was less pronounced, decreasing only by ~30% (Fig. 5E). These altered enzymatic activities demonstrate the importance of *TbFdxA*, but not *TbFdxB*, in the formation of both mitochondrial and cytosolic Fe-S cluster proteins. Threonine dehydrogenase, which lacks Fe-S clusters and was used as a control, remained unaffected in studied cell lines (Fig. S5).

Haem content is decreased in *TbFdxA* knock-down

Haem *a* is a prosthetic group of eukaryotic mitochondrial cytochrome *c* oxidase (complex IV) and some prokaryotic cytochrome oxidases. Complex IV is the only known eukaryotic protein containing haem *a* (Michel *et al.*, 1998;

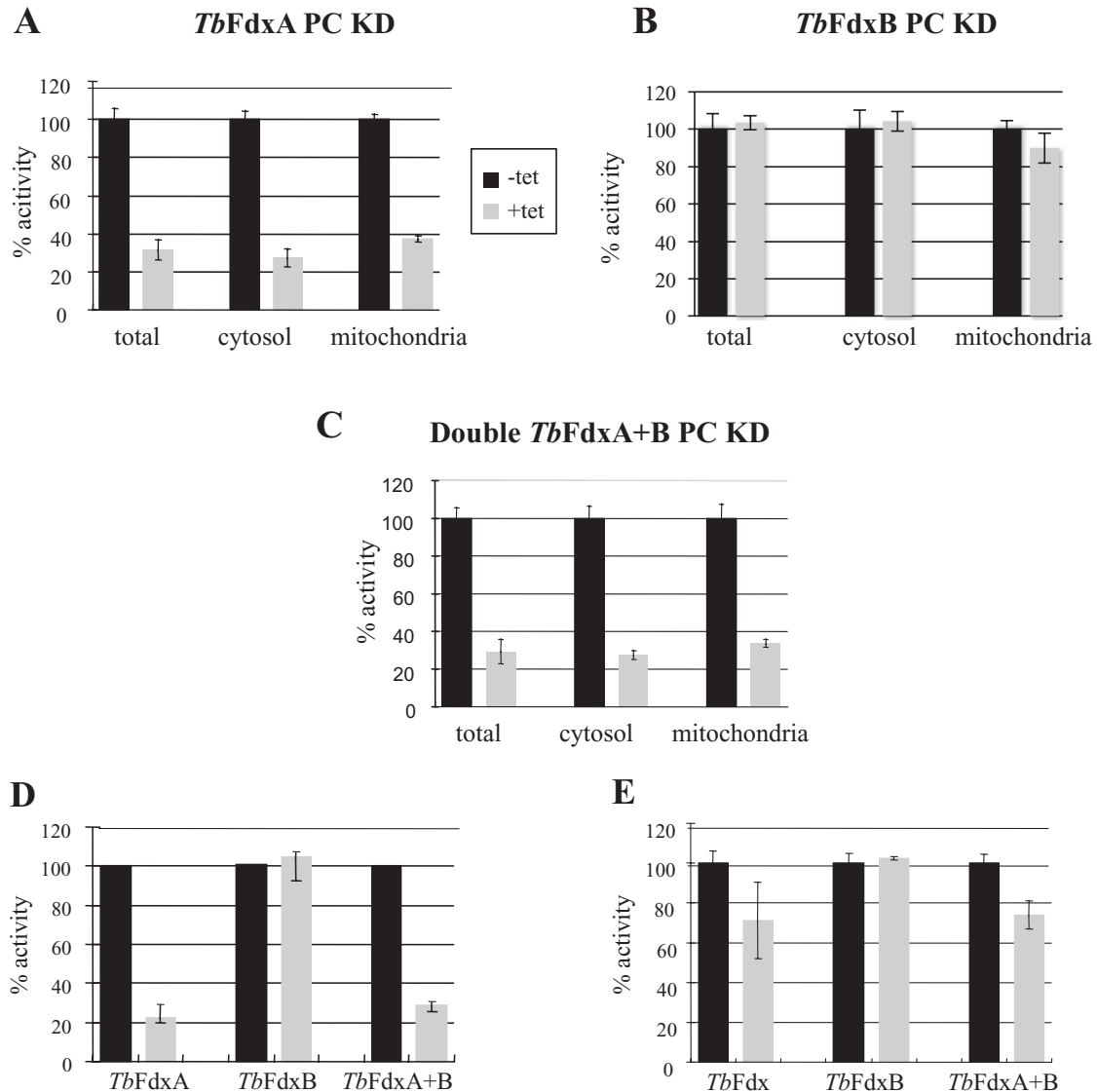


Fig. 5. Effect of *TbFdxA* and *TbFdxB* depletion in PC on Fe-S proteins. Aconitase activities of non-induced (black column) (-Tet) and RNAi-induced (grey column) (+Tet) of single *TbFdxA* (A), single *TbFdxB* (B) and double *TbFdxA+B* knock-down PC cells (C) were measured in whole cell, cytosolic and mitochondrial compartments 5 days after RNAi. Enzymatic activities of succinate dehydrogenase (complex II) (D) and cytochrome *c* reductase (complex III) (E) were measured in crude mitochondrial membrane extract. Specific activities are shown as a percentage of activities in non-induced cells. The means and SD values of three independent experiments are shown.

Barrientos *et al.*, 2009) and as such, bovine heart complex IV was used as a haem *a* standard for HPLC analysis (Fig. 6A). Since in *S. cerevisiae* ferredoxin together with ferredoxin reductase and Cox15 are required for the biosynthesis of haem *a* from the more abundant cellular haem *b* (Barros *et al.*, 2002), we measured the concentrations of haem *a* and haem *b* in the PC trypanosomes with ablated *TbFdxA*. We detected a 20% decrease of both haem *a* and haem *b* as compared with the non-induced cells (Fig. 6B), with the *P*-values being very close to the significant value (haem *b* *P* = 0.0682; haem *a* *P* = 0.0702).

TbFdxA knock-down alters mitochondrial biology

In the PC cells appropriate function of all respiratory complexes is required to maintain mitochondrial inner membrane potential (Besteiro *et al.*, 2005). Membrane potential was drastically reduced in *TbFdxA*-depleted cells, as measured by flow cytometry via quantification of TMRE uptake (Fig. S6A). Furthermore, the same cells accumulated ROS, as followed by dihydroethidium oxidation (Fig. S6B). Extensive disruption of the overall mitochondrial metabolism was reflected in alterations in levels of metabolic end-products upon *TbFdxA* RNAi induction. The

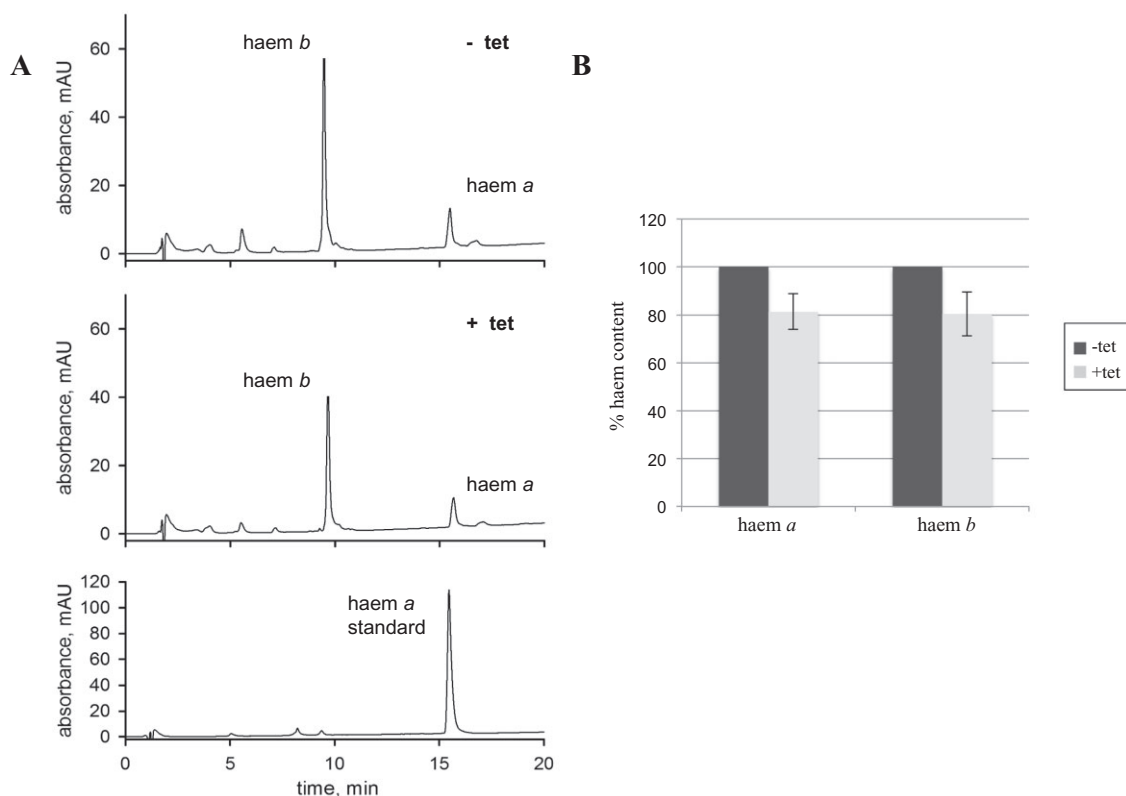


Fig. 6. Haem is decreased in PC *TbFdxA*-depleted cell.

A. Representative measurement of haem of non-induced (–Tet) and RNAi-induced (+Tet) single *TbFdxA* knock-down PC cells. Peaks at 10th and 16th min. represent haem *b* and haem *a* respectively.

B. Amount of haem *a* and haem *b* shown as a percentage with the level in the non-induced cells set to 100%. Dark grey and light grey columns represent per cent haem content of non-induced and RNAi-induced *TbFdxA* PC cells (day 7 post induction) respectively. The means and SD values of four independent RNAi inductions are shown. Haem was extracted from 2×10^9 cells, separated by HPLC and detected by diode array detector. *P*-values were calculated with a non-parametric Student's *t*-test (haem *b* *P* = 0.0682; haem *a* *P* = 0.0702).

most prominent change was an eightfold increase in pyruvate production. In contrast, excretion of succinate and acetate significantly lowered in the induced cells (Fig. S6C and Table S1).

Human ferredoxin homologues rescue *TbFdxA* knock-down

Taking advantage of the *T. brucei* model to gain insight into the controversial function of both human ferredoxin homologues, we tested the ability of each to compensate for the loss of *TbFdxA*. To this end, two rescue cell lines were generated, each constitutively expressing one of the two human ferredoxin genes fused to a C-terminal EGFP tag, which enabled us to monitor their expression (Fig. 7A). In both cell lines, the tagged human ferredoxins (HsFdx1 and HsFdx2) showed a strong signal which colocalized with Mitotracker Red (Fig. 7B). The exclusive mitochondrial localization of these human proteins demonstrated the ability of their respective human mitochondrial targeting

sequences to efficiently mediate import of the downstream protein into the trypanosome mitochondrion (Fig. 7B).

Following RNAi induction, both HsFdx1 and HsFdx2 were able to rescue cell growth, with no growth defect observed throughout the 8-day period for which growth was measured (Fig. 8A), in contrast to the parental *TbFdxA* RNAi line (Fig. 3A). Hence, the presence of either HsFdx1 or HsFdx2 was sufficient to support, in the absence of *TbFdxA*, the growth of PC at wild-type level. Furthermore, aconitase activity in the *TbFdxA*-depleted cells was rescued by HsFdx1 to almost wild-type level in both cytosolic and mitochondrial compartments (Fig. 8B). In the case of HsFdx2, the total aconitase activity was rescued completely, and the mitochondrially localized fraction was even slightly overexpressed (Fig. 8B). Western blot analysis confirmed that about 95% of *TbFdxA* was eliminated within 2 days of RNAi (Fig. 7A). These data demonstrate that either human ferredoxin homologue is sufficient to compensate for the essential Fe-S biosynthetic function of *TbFdxA* in *T. brucei*.

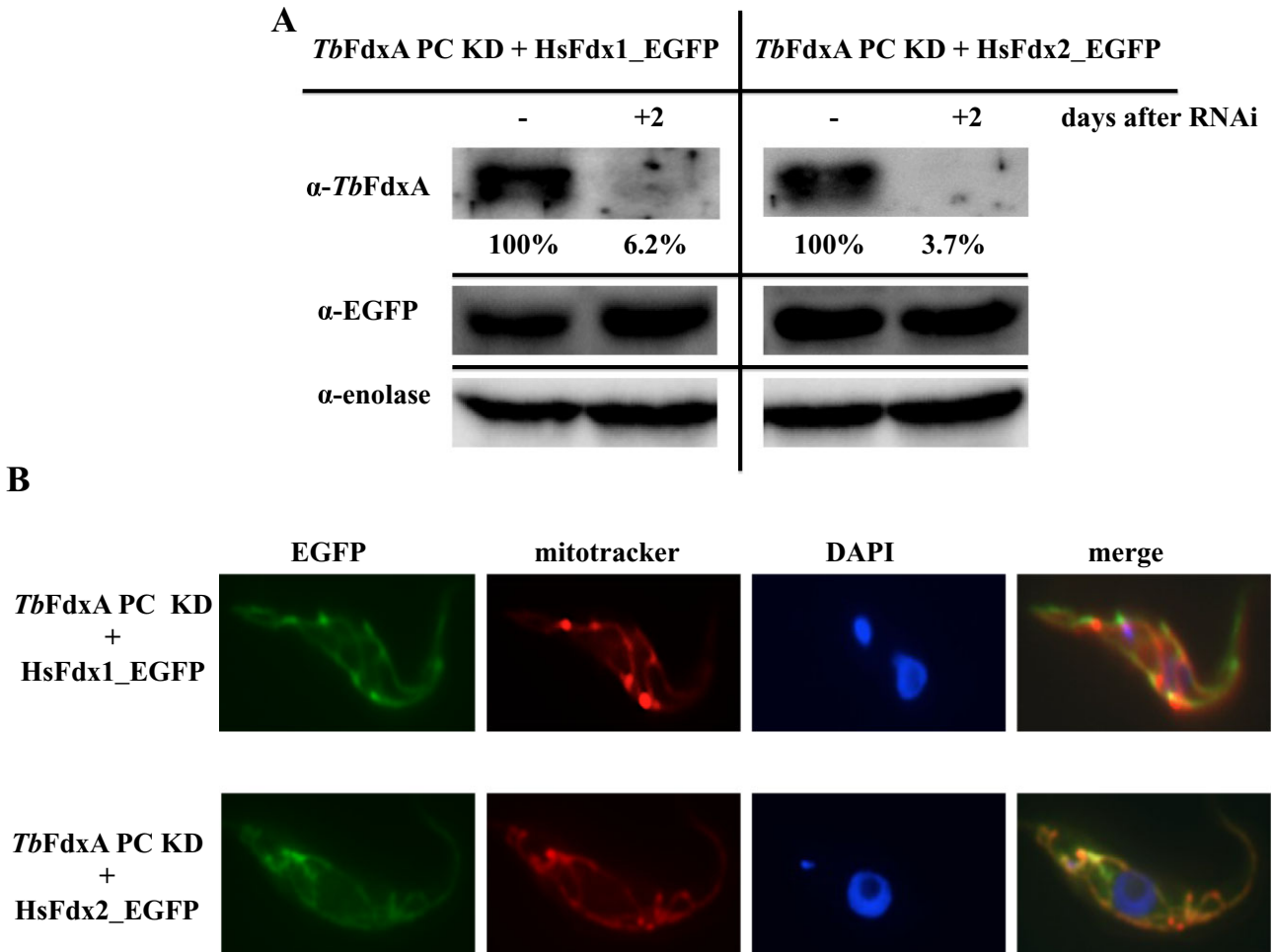


Fig. 7. HsFdx1 and HsFdx2 are expressed in PC *TbFdxA* RNAi cell lines and imported into the *T. brucei* mitochondrion.

A. Western blot analysis with α -*TbFdxA* antibody determines level of endogenous *TbFdxA* 2 days upon RNAi induction. Expression of HsFdx1-EGFP or HsFdx2-EGFP in the *TbFdxA* knock-down cells was followed by α -EGFP antibody. Enolase was used as a loading control. Western blots were quantified with Image J software, enolase was used as a normalizer.

B. Fluorescence microscopy of *TbFdxA* knock-down cell lines expressing HsFdx1-EGFP or HsFdx2-EGFP. Mitotracker Red staining visualizes the mitochondrion. 4,6-diamidino-2-phenylindole (DAPI) stains nuclear and mitochondrial DNA.

Discussion

Ever since ferredoxin was first isolated from *Clostridium pasteurianum* in the early 1960s (Mortenson *et al.*, 1962), this protein highly conserved across the prokaryotic and eukaryotic domains has emerged as a multifunctional protein involved in electron transport, biosynthesis of coenzyme Q, steroid hormone and haem *a* synthesis (Barros *et al.*, 2002; Pierrel *et al.*, 2010; Ewen *et al.*, 2011). Moreover, as both a [2Fe-2S] cluster-containing protein and a Fe-S biosynthetic enzyme, it has the converse properties of being both dependent on and essential for cluster assembly (Barros and Nobrega, 1999; Lange *et al.*, 2000; Tokumoto and Takahashi, 2001).

Here, we have identified two mitochondrial ferredoxin homologues in *T. brucei*, named *TbFdxA* and *TbFdxB*,

and experimentally verified their localization within the organelle. Phylogenetic analysis of ferredoxins across the eukaryotic supergroups revealed that both trypanosome homologues are only distantly related to other ferredoxins and that *TbFdxB* and its homologues in other kinetoplastids constitute the basal branch of the tree. Moreover, this approach detected amplification of ferredoxins in the genomes of *Leishmania* species.

In a recent global RNAi analysis in *T. brucei*, *TbFdxA* was found to be essential in both PC and BS cells, unlike *TbFdxB* which was essential only in the former stage (Alford *et al.*, 2011). Contradictory to this high-throughput screen, the separate and tandem RNAi silencing of ferredoxins presented here showed that *TbFdxA* is essential in both life cycle stages while *TbFdxB*, which we studied only in the PC cells, is dispensable. Moreover, the experi-

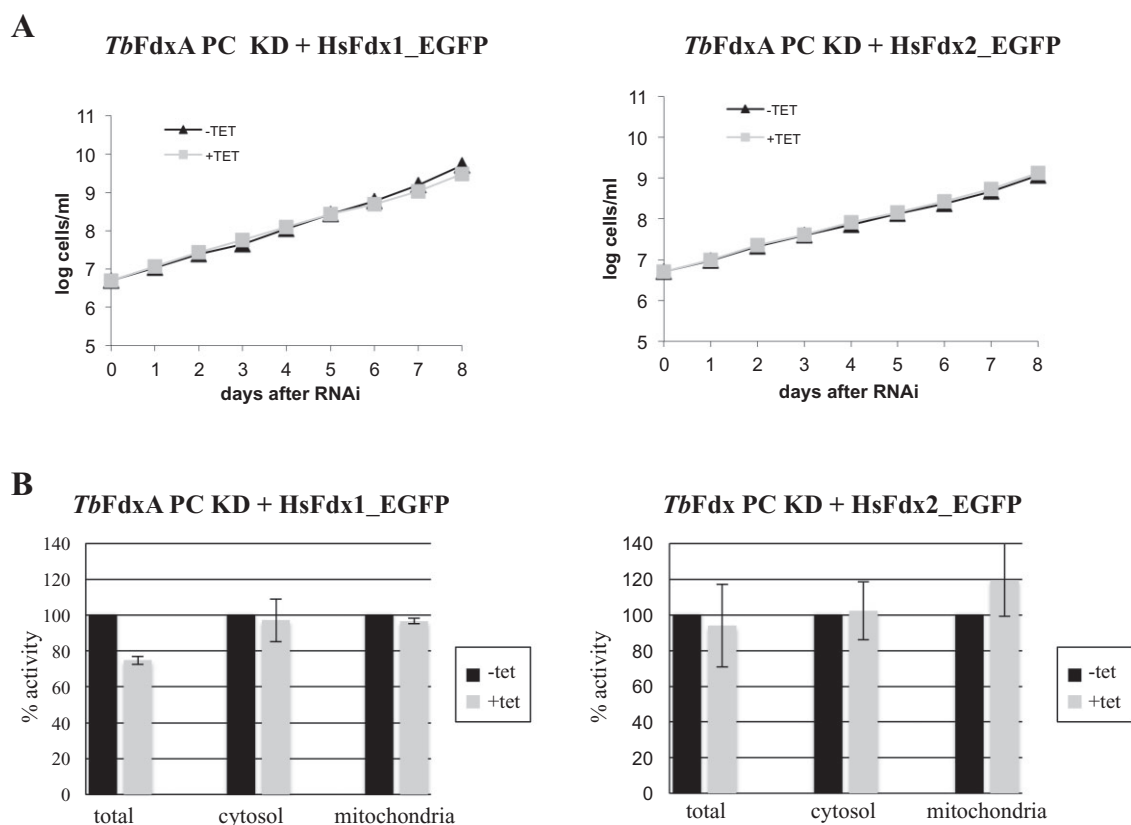


Fig. 8. Expression of either human ferredoxin rescues *TbFdxA* depletion in PC.

A. Growth curves of non-induced (triangle; black line) and RNAi-induced (square; grey line) *TbFdxA* knock-down PC cells constitutively expressing HsFdx1 (left) or HsFdx2 (right). The y-axis represents the log scale product of cell density and total dilution. The data show a single representative experiment of biological triplicates.

B. Aconitase activities in whole cell lysates as well as, cytosolic and mitochondrial compartments of *TbFdxA* knock-down PC cells expressing HsFdx1 (left) or HsFdx2 (right) 5 days post induction. Specific activities are shown for non-induced (black columns) and RNAi-induced cells (grey columns) as a percentage of activity of non-induced cells. The means and SD values of three independent experiments are shown.

mental set-up enabled us to rule out the possibility of redundancy between both homologues.

Upon depletion of *TbFdxA* in the PC cells, the activities of Fe-S cluster-containing cytosolic and mitochondrial aconitase, as well as respiratory complex II were dramatically decreased. Respiratory complex III activity was also reduced, although to a lesser extent. The alterations in the respiratory chain likely caused the decrease of mitochondrial membrane potential and a direct transfer of electrons from complex III to oxygen, with the concomitant production of ROS as was reported recently (Gnipová *et al.*, 2012). These activity measurements confirmed the indispensability of *TbFdxA* in Fe-S cluster biogenesis in both compartments, which is in good correlation with other eukaryotes (Lange *et al.*, 2000; Shi *et al.*, 2012). Since its depletion does not affect levels of frataxin, IscU or Nfs and it was not detected in the IscU/Nfs/Isc11 complex (Paris *et al.*, 2010), *TbFdxA* most likely functions as a solo player that does not stably associate with other ISC assembly proteins. Indeed, exactly how ferredoxin participates in

the Fe-S biosynthesis remains largely unknown. Available data support its function in an electron transfer chain, in which ferredoxin reductase receives electrons from NADH and transfers them to ferredoxin, which in turn donates electrons for the reduction of cysteine-derived sulphur in order to produce the sulphide component of the clusters (Mühlenhoff *et al.*, 2003). Since ablation of *TbFdxB* in PC did not cause any visible phenotype, the function of this unusual ferredoxin, representative of a kinetoplastid-specific branch distinct from all other eukaryotic ferredoxins, remains to be established.

Trypanosomes are unusual among eukaryotes in that they have lost the capacity to synthesize haem *b*, which must consequently be imported from the host or from the medium (Kořený *et al.*, 2010). Conversion of haem *b* to haem *a* has been described for *T. cruzi* and likely also occurs in *T. brucei* (Tripodi *et al.*, 2011). An additional role for ferredoxin in haem *a* synthesis has been demonstrated in yeast (Barros *et al.*, 2002; Moraes *et al.*, 2004), and as HsFdx2 was able to rescue this function in yeast

cells (Sheftel *et al.*, 2010), we examined the effects of *TbFdxA* depletion on haem levels. HPLC analysis of the *TbFdxA* knock-downs showed that haem *a* and surprisingly also haem *b* levels were decreased by approximately a quarter in the RNAi-induced cells as compared with the non-induced ones. The decrease of haem *a* was expected, on the other hand the level of haem *b* should stay unaffected (Barros *et al.*, 2001). We can only speculate that there may be feedback machinery in *T. brucei* that is providing haem *a*/haem *b* equilibrium. It can be particularly important in the mitochondrion, since respiratory complexes are the main consumers of both haems. Disruption of haem homeostasis can lead to increased ROS production with devastating consequences to the cell. Since the change in haem content is rather low, it seems that in *T. brucei*, as in other organisms (Barros *et al.*, 2002), other players participate in haem *a* biosynthesis apart from ferredoxin. In summary, it seems likely that in bridging the two major mitochondrial iron-consuming pathways, namely haem *a* synthesis and Fe-S cluster assembly, this protein is also perfectly positioned to impact on cellular iron homeostasis, as has been observed upon ferredoxin disruption in both yeast and humans (Sheftel *et al.*, 2010; Miao *et al.*, 2011; Shi *et al.*, 2012).

Although the PC trypanosomes rely on L-proline and other amino acids as a source of energy inside the tsetse fly, they will preferentially consume glucose in a glucose-rich medium (Bringaud *et al.*, 2006). Under such conditions, pyruvate is produced glycolytically and subsequently converted to the metabolic end-products succinate, acetate and lactate. In the *TbFdxA*-depleted PC cells, the production of pyruvate dramatically increases. This can be well explained by a compensatory upregulation of glycolysis in response to reduced mitochondrial substrate level ATP production (Bochud-Allemann and Schneider, 2002). Similar phenotype was observed in the PC cells depleted for other Fe-S assembly proteins (Smíd *et al.*, 2006). By decreasing acetate and ATP production, mitochondria of these genetically modified PC act like metabolically suppressed organelles in the BS flagellates. The parallel decrease in succinate production, meanwhile, may result from depletion of its fumarate precursor due to impaired function of the Fe-S-dependent enzyme fumarase, which is required for the conversion of malate to fumarate. Because we observed loss of membrane potential in *TbFdxA* PC KD, pyruvate cannot enter the organelle since it requires H⁺ symport. Nevertheless, even if pyruvate reached the mitochondrial matrix, it cannot be converted to acetyl-CoA, as this reaction requires available NAD⁺. It is unlikely that mitochondrion lacking Fe-S production possesses enough capacity to regenerate this cofactor having respiratory chain off-line. Tentatively, the production of acetate is diminished as a consequence of pyruvate not

being able to reach the mitochondrion and the lack of NAD⁺ available for the pyruvate-acetyl-CoA reaction.

Since the rudimentary mitochondrion of the BS trypanosomes lacks both respiratory chain and tricarboxylic acid cycle (Grant and Sargent, 1960), it is not surprising that its levels of *TbFdxA* are greatly reduced. In fact, the only Fe-S cluster-containing proteins we are aware of in this organelle are monothiol glutaredoxin-1 and aconitase expressed at a very low level (Saas *et al.*, 2000; Comini *et al.*, 2008), while the cytosol of BS contains numerous indispensable proteins, the function of which depends on clusters, such as RLI and nuclear DNA polymerases (Estévez *et al.*, 2004; Netz *et al.*, 2012). Initially, the absence of any growth defect following RNAi-mediated depletion called into question the essentiality of *TbFdxA* for the BS. However, conditional knockout cells provided evidence that even in this life cycle stage, canonical Fe-S cluster assembly takes place within the repressed mitochondrion and the whole pathway thus remains essential. Indeed, ferredoxins are known to be retained in mitochondrion-derived reduced organelles of anaerobic protists, such as the hydrogenosomes of *Trichomonas vaginalis* (Sutak *et al.*, 2004) and the mitosomes of *Giardia intestinalis* (Tovar *et al.*, 2003). Thus, Fe-S cluster biosynthesis clearly remains one of the fundamental processes of mitochondria and mitochondrion-like organelles, the role of which in energy production has been diminished or lost altogether.

Our next aim was to shed light, via complementation studies in trypanosomes, on the function of the human ferredoxins, the role of which still remains to some extent controversial. A recent study in yeast demonstrated that only HsFdx2 but not HsFdx1 can complement the defect in Fe-S cluster assembly in the yeast Yah1 mutant (Sheftel *et al.*, 2010). In contrast, another group showed that both human ferredoxins together with ferredoxin reductase are involved in Fe-S cluster assembly (Shi *et al.*, 2012). We took advantage of the PC knock-downs to perform complementation assays with two EGFP-tagged human ferredoxins, equipped with their endogenous mammalian mitochondrial import signals. Interestingly, both human proteins mediated a full rescue in terms of growth defect and aconitase activity. These successful rescues strongly support the view that the human ferredoxins are functional homologues that evolved by gene duplication.

The highly efficient import of both human proteins via their genuine import signals is unexpected and exciting on its own right, since trypanosomes and humans shared the last common ancestor perhaps over 1 billion years ago, and these flagellates qualify for one of the earliest offshoots of the eukaryotic tree (Cavalier-Smith, 2010). Moreover, trypanosomes and related flagellates are characterized by generally very short mitochondrial import presequences (Schneider *et al.*, 2008) and elusive trans-

porters of the inner and outer membrane complexes. This may be caused by either genuine absence of most key subunits (Pusnik *et al.*, 2009), divergence obscuring their recognition (Žárský *et al.*, 2012), or the existence of transporter complexes that are mostly composed of novel proteins (Singha *et al.*, 2012). It has been shown previously in *T. brucei* that the mitochondrial presequence of human frataxin is sufficient for import and processing of human frataxin (Long *et al.*, 2008) and human Isa1/2 proteins (Long *et al.*, 2011). Our corresponding finding for HsFdx1 and HsFdx2 suggests that the *T. brucei* mitochondrion is capable of importing proteins with complex organellar import signals.

Experimental procedures

Phylogenetic analysis

Maximum likelihood phylogeny of the aligned data set was created using RAxML 7.3a (Stamatakis, 2006) employing Γ -corrected LG substitution matrix. The highest scoring topology was chosen from 100 independent runs each starting with a different starting tree. Branching support was assessed using non-parametric bootstrapping (RAxML LG+ Γ ; 500 replicates) and Bayesian posterior probabilities as estimated in Phylobayes 3.2 (Lartillot *et al.*, 2009) under the empirical mixture model C40 combined with substitution rates derived from the LG matrix. For this, two independent chains were run until their maximum observed discrepancy was lower than 0.1 (i.e. they converged) and effective sample size of model parameters was equal to 150 or higher.

Preparation of pT7V5-FdxA and pT7V5-FdxB constructs

Gene constructs were prepared to contain *TbFdxA* (Tb927.7.890) and *TbFdxB* (Tb927.4.4980) ORFs lacking stop codons followed by V5 tags. They were amplified from the total genomic DNA of *T. brucei* strain 29-13 using primer pairs *TbFdxA_V5-FP* (5'-CGCAAAGCTTATGGCTGCTTTA CGCTACTT) and *TbFdxA_V5-RP* (5'-CGCGGATCCGTGA TGAGGGTTATGGTGT), and *TbFdxB_V5-FP* (5'-CGCAA GCTTATGCTTTCCGCAACTTTCGG) and *TbFdxB_V5-RP* (5'-CGCGGATCCCGCATTTCATTTCGTTGTTT) (added BamHI and HindIII restriction sites are underlined).

PCR product were cloned into pT7V5 vector and verified by sequencing. The pT7V5-FdxA and pT7V5-FdxB were linearized with NotI and electroporated into wild-type PC *T. brucei* strain 29-13. The transfected cell lines were selected on puromycin ($1 \mu\text{g ml}^{-1}$) and expression of the tagged protein was induced by addition of Tet ($1 \mu\text{g ml}^{-1}$).

RNAi constructs, transfections, cloning, RNAi induction and cultivation

To prepare *TbFdxA* (Tb927.7.890) and *TbFdxB* (Tb927.4.4980) RNA interference (RNAi) constructs, 537-nt-long and 504-nt-long fragments of *TbFdxA* and *TbFdxB* respectively, were amplified using primer pairs *TbFdxA-FP* (5'-GAAG

CTTATGGCTGCTTACGCTACTT) and *TbFdxA-RP* (5'-GACTAGTTCAGTGATGAGGGGTTATGG), and *TbFdxB-FP* (5'-GAAGCTTATGCTTTCCGCAACTTTCGG) and *TbFdxB-RP* (5'-GACTAGTTCACCGCATTTCATTTCGTTG) (added HindIII and SpeI restriction sites are underlined) and total genomic DNA of *T. brucei* strain 29-13 as a template. Both amplicons were separately cloned into the p2T7-177 vector which was, upon NotI-mediated linearization, introduced into PC *T. brucei* 29-13 cells using a BTX electroporator and selected as described elsewhere (Vondrušková *et al.*, 2005). The double knock-down was prepared by cloning the amplicon produced by the primers *TbFdxB2KD-FP* (5'-GATCGATATGCTTTCCGCAACTTTCGG) and *TbFdxB2KD-RP* (5'-GCTCGAGTCAACCGCATTTCATTTCGTTG) (added ClaI and XhoI restriction sites are underlined), into the p2T7-177 + *TbFdxA* construct, which was then stably integrated into the PC cells as described above. The p2T7-177 + *TbFdxA* construct was also transfected into BS *T. brucei* 427 cells using the Amaxa Nucleofector II electroporator, with transfectants maintained in HMI-9 medium and selected following a protocol described previously (Hashimi *et al.*, 2008). PC and BS trypanosomes were cultivated in SDM-79 medium at 27°C and HMI-9 medium at 37°C respectively. RNAi was initiated by the addition of $1 \mu\text{g ml}^{-1}$ tetracycline (Tet) to the medium and growth measurements were made using the Beckman Z2 Coulter counter at 24 h intervals, for 9 days in the case of PC and 7 days for BS cells.

Generation of *TbFdxA* conditional knockout

A *TbFdxA* conditional knockout was generated in BS cells strain 427 following a strategy described by Schnauer *et al.* (2001). Fragments of the 5'UTR and 3'UTR of *TbFdxA* were amplified from *T. brucei* genomic DNA using primer pairs 5'UTR-FP (5'-AGTGCGGCCGAGTGGGGCCTGTGGTGT) and 5'UTR-RP (5'-AGTACGCGCTCGAGTGCCCCGCTCA CCT), and 3'UTR-FP (5'-CACTCTAGAATTTAAATCGCAC CCGCCGTAG) and 3'UTR-RP (5'-AGTAGGCCTGCGGC CGCTGGGTGCCTCGCTCA). The amplicons were cloned into the T7RNP/NEO cassette of pLew13. This construct (designated pFdxA-KO1) was then transfected to generate the first allele replacement. Next, pLew79 with full-length *TbFdxA*, PCR-amplified from genomic DNA using primers *FdxAORF-FP* (5'-CACGATTTCATGGCTGCTTTAC) and *FdxAORF-RP* (5'-CACAAGCTTTCAGTGATGAGG), was transfected in order to express an ectopic copy of *TbFdxA* in the presence of Tet. Lastly, pFdxA-KO2 was created by replacing the T7RNP/NEO cassette in pFdxA-KO1 with the TETR/HYG cassette from pLew90. Integration of this plasmid generated the second allele replacement. PCR using primers 5'UTR-FP, *FdxAORF-FP* and *FdxAORF-RP* were used to confirm proper integration in the conditional knockout cells.

Preparation of antibodies and Western blot analysis

The full-size *TbFdxA* and *TbFdxB* genes were amplified by PCR with primers *TbFdxA-FP/O* (5'-CACCATGGCTGCTT TACGCTACTT) and *TbFdxA-RP/O* (5'-TCAGTGATGAGG GGTTATGG), and *TbFdxB-FP/O* (5'-CACCATGCTTTCCGC AACTTTCGG) and *TbFdxB-RP/O* (5'-TCACCGCATTCA

TTCGTTG). The amplicons were gel-purified and cloned into the pET/100D expression vector (Invitrogen). The resulting expression plasmids encoding His₆-tagged *TbFdxA* and *TbFdxB* were transformed into the *E. coli* strain BL21 star (DE3) (Invitrogen). Insoluble proteins were obtained from induced bacterial cells (incubation at 37°C for 3 h; induced with 1 mM IPTG) under denaturing conditions using ProBond Ni-chelating resin (Invitrogen). Polyclonal antibodies against the *TbFdxA* protein were prepared by Cocalico Biologicals (Reamstown, PA, USA) by immunizing a rat at 2-week intervals with the purified recombinant *TbFdxA* protein. Cell lysates corresponding to 5×10^6 cells per lane were separated on a 15% SDS-polyacrylamide gel, transferred to a PVDF membrane and probed. α -*TbFdxA* polyclonal rat antibodies, polyclonal antibodies against enolase (provided by Paul A. M. Michels) and monoclonal antibodies against GFP (Invitrogen) were used at 1:1000, 1:200 000 and 1:1000 dilutions respectively, followed by appropriate secondary antibodies conjugated with horseradish peroxidase (Sigma), then visualized using an ECL kit (Pierce).

Quantitative real-time PCR

Total RNA from induced and non-induced cells was isolated using TRIzol (Sigma). The turbo DNA-free DNase kit (Ambion) was used to remove residual DNA. Reverse transcription using the SuperScript III reverse transcriptase (Invitrogen) and Oligo (dT)₂₀ primer (Invitrogen) was performed to obtain cDNAs. Quantitative real-time PCR reactions were performed as described elsewhere (Hashimi *et al.*, 2008). The primer pair for detecting of *TbFdxB* mRNA is *FdxB-qPCR-FW* (5'-TGCCAGGTAAAGCTCAGCAA) and *TbFdxB_V5-RP*. The primer pair for the internal reference 18S rRNA was described previously (Carnes *et al.*, 2005). The relative *TbFdxB* mRNA abundance between induced and non-induced cells was determined by the Pfaffl method (Pfaffl, 2001).

Digitonin fractionation and enzymatic activities measurement

Cytosolic and mitochondrial fractions for aconitase activity measurements were obtained by digitonin fractionation, performed as described elsewhere (Smíd *et al.*, 2006). Total cell fraction was obtained by treating cell suspension in Hanks' balanced salt solution with 0.1% Triton X-100 and incubating for 5 min. After centrifugation the supernatant was collected as total cell fraction. Aconitase activity was measured spectrophotometrically at 240 nm as production of *cis*-aconitate. The activity of threonine dehydrogenase was measured at 340 nm as a rate of NAD reduction. The activities of succinate dehydrogenase and cytochrome *c* reductase were measured in crude mitochondrial membrane extract as described elsewhere (Horváth *et al.*, 2005).

Measurement of mitochondrial inner membrane potential and ROS

Approximately 5×10^6 cells of exponentially growing PC *T. brucei* were harvested and centrifuged, and the pellet was

resuspended in 1 ml fresh SDM-79 medium. Membrane potential was measured by monitoring uptake of tetramethylrhodamine ethyl ester (TMRE) (Molecular Probes) as described previously (Horváth *et al.*, 2005). Reactive oxygen species (ROS) were measured by oxidation of dihydroethidium (Sigma) as described elsewhere (Long *et al.*, 2008). After staining with $5 \mu\text{g ml}^{-1}$ dihydroethidium for 30 min at 27°C, cells were resuspended in 5 ml iso-flow buffer. Intracellular ROS were detected by an Epics XL flow cytometer (Beckman Coulter) with excitation and emission settings of 488 nm and 620 nm respectively.

Determination of metabolic end-products

Approximately 8×10^7 cells were washed with incubation buffer (PBS supplemented with 11 mM glucose and 24 mM NaHCO₃, pH 7.3). After incubation for 2 h at 27°C, cells were centrifuged for 10 min at 3000 r.p.m. The supernatant was collected and analysed by HPLC in a PL Hi-Plex H column as described elsewhere (Vaňáčová *et al.*, 2001).

Immunofluorescence assay

Approximately 1×10^7 PC cells were collected, centrifuged, resuspended in fresh medium and stained with 200 nM of the mitochondrion-selective dye Mitotracker Red (Invitrogen). After 30 min incubation at 27°C, the cells were centrifuged for 5 min at 3000 r.p.m. at room temperature. The pellet was washed and resuspended in 1 ml PBS with 4% paraformaldehyde and 1.25 mM NaOH. Two hundred and fifty microlitres of the suspension was applied to a microscopic slide and incubated for 10 min at room temperature. The slides were washed with PBS, incubated in ice-cold methanol for an additional 20 min and washed briefly with PBS. Primary anti-V5 antibody (Invitrogen) was added at 1:100 dilution in PBS-Tween (0.05%) with 5% milk and incubated at 4°C overnight. Slides were washed with PBS. Alexa Fluor® 488 goat anti-mouse IgG (Molecular Probes) was used at 1:1000 dilution for 1 h at room temperature. The samples were mounted with antifade reagent with DAPI (Invitrogen). After incubation in the dark for 30 min, the sample was visualized using an Axioplan2 imaging (Zeiss) fluorescent microscope.

Human ferredoxin rescues and growth curves

To prepare constructs expressing human ferredoxin, the *HsFdx1* and *HsFdx2* genes, each conjugated to C-terminal enhanced green fluorescent protein (EGFP), were amplified from the *HsFdx1*-EGFP-N3 and *HsFdx2*-EGFP-N3 plasmids respectively (kindly provided by Antonio Pierik and Roland Lill). PCR was performed using primer *huFdx1-1* (5'-AAGCTTATGGCTGCCGCTGGGGCGC) or *huFdx2-F* (5'-AAGCTTGCTACCGGACTCAGATCTAC) in combination with common *huFdx-R* (5'-GATATCTTTACTTGACAGCTCGTCCA) (added restriction sites HindIII and EcoRV are underlined). Each product was cloned into the pABPURO constitutive expression vector. The *HsFdx1*-EGFP-pABPURO and *HsFdx2*-EGFP-pABPURO constructs were separately transfected into PC cells carrying the inducible *TbFdxA* RNAi construct. Transformants were selected with puromycin and

clonal cell lines were obtained by limiting dilution. RNAi was induced with the addition of Tet and growth measurements were made using the Beckman Z2 Coulter counter at 24 h intervals for 8 days.

Haem measurement

A total of 2×10^9 PC cells were harvested, centrifuged at 3000 r.p.m. for 5 min and washed three times with PBS. The cell pellet was then resuspended in 200 μ l H₂O and extracted with 400 μ l acetone/0.2% HCl. The supernatant was collected after centrifugation for 5 min at 12 000 r.p.m. The pellet was resuspended in 300 μ l acetone/0.2% HCl and spun again for 5 min at 12 000 r.p.m. Both supernatants were combined and 150 μ l of each sample was separated by HPLC on a Nova-Pak C18 column using linear gradient 25–100% acetonitrile/0.1% trifluoroacetic acid at a flow rate of 1.1 ml min⁻¹ at 40°C. Haem was detected by diode array detector Agilent 1200 (Agilent Technologies).

Acknowledgements

We thank Roman Sobotka (Institute of Microbiology, Třeboň) for valuable help with the HPLC experiment, Antonio Pierik and Roland Lill (Philipps University, Marburg) for kindly sharing plasmids with tagged human ferredoxins, Aleš Horák (Biology Centre, České Budějovice) for help with phylogenetic analysis, Ivan Hrdý (Charles University, Prague) for end-product measurement, Luděk Kořený (University of Cambridge, Cambridge) and Zdeněk Verner (Comenius University, Bratislava) for helpful discussions and Paul A. M. Michels (Universidad de los Andes, Mérida) for the gift of α -enolase antibodies. This work was supported by the Grant Agency of the Czech Republic (P305/11/2179), Czech Ministry of Education (AMVIS LH12104), and the Praemium Academiae award to J.L., who is also a Fellow of the Canadian Institute for Advanced Research.

References

- Adam, A.C., Bornhvd, C., Prokisch, H., Neupert, W., and Hell, K. (2006) The Nfs1 interacting protein Isd11 has an essential role in Fe/S cluster biogenesis in mitochondria. *EMBO J* **25**: 174–183.
- Alsford, S., Turner, D.J., Obado, S.O., Sanchez-Flores, A., Glover, L., Berriman, M., *et al.* (2011) High-throughput phenotyping using parallel sequencing of RNA interference targets in the African trypanosome. *Genome Res* **21**: 915–924.
- Barrientos, A., Gouget, K., Horn, D., Soto, I.C., and Fontanesi, F. (2009) Suppression mechanisms of COX assembly defects in yeast and human: insights into the COX assembly process. *Biochim Biophys Acta* **1793**: 97–107.
- Barros, M.H., and Nobrega, F.G. (1999) YAH1 of *Saccharomyces cerevisiae*: a new essential gene that codes for a protein homologous to human adrenodoxin. *Gene* **233**: 197–203.
- Barros, M.H., Carlson, C.G., Glerum, D.M., and Tzagoloff, A. (2001) Involvement of mitochondrial ferredoxin and Cox15p in hydroxylation of heme O. *FEBS Lett* **492**: 133–138.
- Barros, M.H., Nobrega, F.G., and Tzagoloff, A. (2002) Mitochondrial ferredoxin is required for heme A synthesis in *Saccharomyces cerevisiae*. *J Biol Chem* **277**: 9997–10002.
- Besteiro, S., Biran, M., Biteau, N., Coustou, V., Baltz, T., Canioni, P., and Bringaud, F. (2002) Succinate secreted by *Trypanosoma brucei* is produced by a novel and unique glycosomal enzyme, NADH-dependent fumarate reductase. *J Biol Chem* **277**: 38001–38012.
- Besteiro, S., Barrett, M., Riviere, L., and Bringaud, F. (2005) Energy generation in insect stages of *Trypanosoma brucei*: metabolism in flux. *Trends Parasitol* **21**: 185–191.
- Bochud-Allemann, N., and Schneider, A. (2002) Mitochondrial substrate level phosphorylation is essential for growth of procyclic *Trypanosoma brucei*. *J Biol Chem* **277**: 32849–32854.
- Bringaud, F., Riviere, L., and Coustou, V. (2006) Energy metabolism of trypanosomatids: adaptation to available carbon sources. *Mol Biochem Parasitol* **149**: 1–9.
- Bruhn, D.F., Sammartino, M., and Klingbeil, M.M. (2011) Three mitochondrial DNA polymerases are essential for kinetoplast DNA replication and survival of bloodstream form *Trypanosoma brucei*. *Eukaryot Cell* **10**: 734–743.
- Carnes, J., Trotter, J.R., Ernst, N.L., Steinberg, A., and Stuart, K. (2005) An essential RNase III insertion editing endonuclease in *Trypanosoma brucei*. *Proc Natl Acad Sci USA* **102**: 16614–16619.
- Cavalier-Smith, T. (2010) Deep phylogeny, ancestral groups and the four ages of life. *Philos Trans R Soc Lond B Biol Sci* **365**: 111–132.
- Chandramouli, K., Unciuleac, M.C., Naik, S., Dean, D.R., Huynh, B.H., and Johnson, M.K. (2007) Formation and properties of [4Fe-4S] clusters on the IscU scaffold protein. *Biochemistry* **46**: 6804–6811.
- Comini, M.A., Rettig, J., Dirdjaja, N., Hanschmann, E.M., Berndt, C., and Krauth-Siegel, R.L. (2008) Monothiol glutaredoxin-1 is an essential iron-sulfur protein in the mitochondrion of African trypanosomes. *J Biol Chem* **283**: 27785–27798.
- Coustou, V., Biran, M., Besteiro, S., Riviere, L., Baltz, T., Franconi, J.M., and Bringaud, F. (2006) Fumarate is an essential intermediary metabolite produced by the procyclic *Trypanosoma brucei*. *J Biol Chem* **281**: 26832–26846.
- Estévez, A.M., Haile, S., Steinbuchel, M., Quijada, L., and Clayton, C. (2004) Effects of depletion and overexpression of the *Trypanosoma brucei* ribonuclease L inhibitor homologue. *Mol Biochem Parasitol* **133**: 137–141.
- Ewen, K.M., Kleser, M., and Bernhardt, R. (2011) Adrenodoxin: the archetype of vertebrate-type [2Fe-2S] cluster ferredoxins. *Biochim Biophys Acta Proteins Proteomics* **1814**: 111–125.
- Gnipová, A., Panicucci, B., Paris, Z., Verner, Z., Horváth, A., Lukeš, J., and Zíková, A. (2012) Disparate phenotypic effects from the knockdown of various *Trypanosoma brucei* cytochrome c oxidase subunits. *Mol Biochem Parasitol* **184**: 90–98.
- Grant, P.T., and Sargent, J.R. (1960) Properties of L- α -glycerophosphate oxidase and its role in the respiration of *Trypanosoma rhodesiense*. *Biochem J* **76**: 229–237.
- Hashimi, H., Zíková, A., Panigrahi, A.K., Stuart, K.D., and Lukeš, J. (2008) TbRGG1, an essential protein involved in

- kinetoplastid RNA metabolism that is associated with a novel multiprotein complex. *RNA* **14**: 970–980.
- Horváth, A., Horáková, E., Dunajčíková, P., Verner, Z., Pravdová, E., Šlapetová, I., et al. (2005) Downregulation of the nuclear-encoded subunits of the complexes III and IV disrupts their respective complexes but not complex I in procyclic *Trypanosoma brucei*. *Mol Microbiol* **58**: 116–130.
- Kakuta, Y., Horio, T., Takahashi, Y., and Fukuyama, K. (2001) Crystal structure of *Escherichia coli* Fdx, an adrenodoxin-type ferredoxin involved in the assembly of iron-sulfur clusters. *Biochemistry* **40**: 11007–11012.
- Kořený, L., Lukeš, J., and Oborník, M. (2010) Evolution of the haem synthetic pathway in kinetoplastid flagellates: an essential pathway that is not essential after all? *Int J Parasitol* **40**: 149–156.
- Lange, H., Kaut, A., Kispal, G., and Lill, R. (2000) A mitochondrial ferredoxin is essential for biogenesis of cellular iron-sulfur proteins. *Proc Natl Acad Sci USA* **97**: 1050–1055.
- Lartillot, N., Lepage, T., and Blanquart, S. (2009) PhyloBayes 3: a Bayesian software package for phylogenetic reconstruction and molecular dating. *Bioinformatics* **25**: 2286–2288.
- Li, J., Saxena, S., Pain, D., and Dancis, A. (2001) Adrenodoxin reductase homolog (Arh1p) of yeast mitochondria required for iron homeostasis. *J Biol Chem* **276**: 1503–1509.
- Lill, R. (2009) Function and biogenesis of iron-sulphur proteins. *Nature* **460**: 831–838.
- Long, S., Jirků, M., Ayala, F.J., and Lukeš, J. (2008) Mitochondrial localization of human frataxin is necessary but processing is not for rescuing frataxin deficiency in *Trypanosoma brucei*. *Proc Natl Acad Sci USA* **105**: 13468–13473.
- Long, S.J., Changmai, P., Tsaousis, A.D., Skalický, T., Verner, Z., Wen, Y.Z., et al. (2011) Stage-specific requirement for Isa1 and Isa2 proteins in the mitochondrion of *Trypanosoma brucei* and heterologous rescue by human and *Blasotocystis* orthologues. *Mol Microbiol* **81**: 1403–1418.
- Lukeš, J., Hashimi, H., and Ziková, A. (2005) Unexplained complexity of the mitochondrial genome and transcriptome in kinetoplastid flagellates. *Curr Genet* **48**: 277–299.
- Marchler-Bauer, A., Lu, S., Anderson, J.B., Chitsaz, F., Derbyshire, M.K., DeWeese-Scott, C., et al. (2011) CDD: a Conserved Domain Database for the functional annotation of proteins. *Nucleic Acids Res* **39**: 225–229.
- Miao, R., Holmes-Hampton, G., and Lindahl, P.A. (2011) Biophysical Investigation of the Iron in Aft1-1(up) and Gal-YAH1 *Saccharomyces cerevisiae*. *Biochemistry* **50**: 2660–2671.
- Michel, H., Behr, J., Harrenga, A., and Kannt, A. (1998) Cytochrome C oxidase: structure and spectroscopy. *Annu Rev Biophys Biomol Struct* **27**: 329–356.
- Moraes, C.T., Diaz, F., and Barrientos, A. (2004) Defects in the biosynthesis of mitochondrial heme c and heme a in yeast and mammals. *Biochim Biophys Acta Bioenerg* **1659**: 153–159.
- Mortenson, L.E., Carnahan, J.E., and Valentine, R.C. (1962) An electron transport factor from *Clostridium pasteurianum*. *Biochem Biophys Res Commun* **7**: 448–452.
- Mühlenhoff, U., Gerber, J., Richhardt, N., and Lill, R. (2003) Components involved in assembly and dislocation of iron-sulfur clusters on the scaffold protein Isu1p. *EMBO J* **22**: 4815–4825.
- Mühlenhoff, U., Gerl, M.J., Flauger, B., Pimer, H.M., Balsler, S., Richhardt, N., et al. (2007) The iron-sulfur cluster proteins Isa1 and Isa2 are required for the function but not for the *de novo* synthesis of the Fe/S clusters of biotin synthase in *Saccharomyces cerevisiae*. *Eukaryot Cell* **6**: 753–753.
- Netz, D.J.A., Stiith, C.M., Stumpfig, M., Kopf, G., Vogel, D., Genau, H.M., et al. (2012) Eukaryotic DNA polymerases require an iron-sulfur cluster for the formation of active complexes. *Nature Chem Biol* **8**: 125–132.
- Paris, Z., Changmai, P., Rubio, M.A., Zíková, A., Stuart, K.D., Alfonzo, J.D., and Lukeš, J. (2010) The Fe/S cluster assembly protein Isd11 is essential for tRNA thiolation in *Trypanosoma brucei*. *J Biol Chem* **285**: 22394–22402.
- Pfaffl, M.W. (2001) A new mathematical model for relative quantification in real-time RT-PCR. *Nucleic Acids Res* **29**: e45.
- Pierrel, F., Hamelin, O., Douki, T., Kieffer-Jaquinod, S., Mühlenhoff, U., Ozeir, M., et al. (2010) Involvement of mitochondrial ferredoxin and para-aminobenzoic acid in yeast coenzyme Q biosynthesis. *Chem Biol* **17**: 449–459.
- Pusnik, M., Charrière, F., Mäser, P., Waller, R.F., Dagley, M.J., Lithgow, T., and Schneider, A. (2009) The single mitochondrial porin of *Trypanosoma brucei* is the main metabolite transporter in the outer mitochondrial membrane. *Mol Biol Evol* **26**: 671–680.
- Py, B., and Barras, F. (2010) Building Fe-S proteins: bacterial strategies. *Nat Rev Microbiol* **8**: 436–446.
- Rouault, T.A. (2012) Biogenesis of iron-sulfur clusters in mammalian cells: new insights and relevance to human disease. *Dis Model Mech* **5**: 155–164.
- Saas, J., Ziegelbauer, K., von Haeseler, A., Fast, B., and Boshart, M. (2000) A developmentally regulated aconitase related to iron-regulatory protein-1 is localized in the cytoplasm and in the mitochondrion of *Trypanosoma brucei*. *J Biol Chem* **275**: 2745–2755.
- Schnauffer, A., Panigrahi, A.K., Panicucci, B., Igo, P., Wirtz, E., Salavati, R., and Stuart, K. (2001) An RNA ligase essential for RNA editing and survival of the bloodstream form of *Trypanosoma brucei*. *Science* **291**: 2159–2162.
- Schneider, A., Bursać, D., and Lithgow, T. (2008) The direct route: a simplified pathway for protein import into the mitochondrion of trypanosomes. *Trends Cell Biol* **18**: 12–18.
- Seeber, F. (2002) Eukaryotic genomes contain a [2Fe-2S] ferredoxin isoform with a conserved C-terminal sequence motif. *Trends Biochem Sci* **27**: 545–547.
- Sheftel, A.D., Stehling, O., Pierik, A.J., Elsasser, H.P., Mühlenhoff, U., Webert, H., et al. (2010) Humans possess two mitochondrial ferredoxins, Fdx1 and Fdx2, with distinct roles in steroidogenesis, heme, and Fe/S cluster biosynthesis. *Proc Natl Acad Sci USA* **107**: 11775–11780.
- Shi, Y.B., Ghosh, M.C., Tong, W.H., and Rouault, T.A. (2009) Human ISD11 is essential for both iron-sulfur cluster assembly and maintenance of normal cellular iron homeostasis. *Hum Mol Genet* **18**: 3014–3025.
- Shi, Y.B., Ghosh, M., Kovtunovych, G., Crooks, D.R., and Rouault, T.A. (2012) Both human ferredoxins 1 and 2 and ferredoxin reductase are important for iron-sulfur cluster

- biogenesis. *Biochim Biophys Acta Mol Cell Res* **1823**: 484–492.
- Singha, U.K., Hamilton, V., Duncan, M.R., Weems, E., Tripathi, M.K., and Chaudhuri, M. (2012) Protein translocase of mitochondrial inner membrane in *Trypanosoma brucei*. *J Biol Chem* **287**: 14480–14493.
- Smíd, O., Horáková, E., Vilimová, V., Hrdý, I., Cammack, R., Horváth, A., *et al.* (2006) Knock-downs of iron-sulfur cluster assembly proteins IscS and IscU down-regulate the active mitochondrion of procyclic *Trypanosoma brucei*. *J Biol Chem* **281**: 28679–28686.
- Stamatakis, A. (2006) RAxML-VI-HPC: maximum likelihood-based phylogenetic analyses with thousands of taxa and mixed models. *Bioinformatics* **22**: 2688–2690.
- Stemmler, T.L., Lesuisse, E., Pain, D., and Dancis, A. (2010) Frataxin and mitochondrial FeS cluster biogenesis. *J Biol Chem* **285**: 26737–26743.
- Sutak, R., Doležal, P., Fiumera, H.L., Hrdý, I., Dancis, A., Delgadillo-Correa, M., *et al.* (2004) Mitochondrial-type assembly of FeS centers in the hydrogenosomes of the amitochondriate eukaryote *Trichomonas vaginalis*. *Proc Natl Acad Sci USA* **101**: 10368–10373.
- Tielens, A.G., and Van Hellemond, J.J. (1998) The electron transport chain in anaerobically functioning eukaryotes. *Biochim Biophys Acta* **1365**: 71–78.
- Tokumoto, U., and Takahashi, Y. (2001) Genetic analysis of the *isc* operon in *Escherichia coli* involved in the biogenesis of cellular iron-sulfur protein. *J Biochem (Tokyo)* **130**: 63–71.
- Tovar, J., Leon-Avila, G., Sanchez, L.B., Šuták, R., Tachezy, J., van der Giezen, M., *et al.* (2003) Mitochondrial remnant organelles of *Giardia* function in iron-sulphur protein maturation. *Nature* **426**: 172–176.
- Tripodi, K.E., Menendez, S.M., and Cricco, J.A. (2011) Role of heme and heme-proteins in trypanosomatid essential metabolic pathways. *Enzyme Res* **2011**: 873230.
- Tsaousis, A.D., de Choudens, S.O., Gentekaki, E., Long, S.J., Gaston, D., Stechmann, A., *et al.* (2012) Evolution of Fe/S cluster biogenesis in the anaerobic parasite *Blastocystis*. *Proc Natl Acad Sci USA* **109**: 10426–10431.
- Vaňáčová, S., Rasoloson, D., Razga, J., Hrdý, I., Kulda, J., and Tachezy, J. (2001) Iron-induced changes in pyruvate metabolism of *Tritrichomonas foetus* and involvement of iron in expression of hydrogenosomal proteins. *Microbiology* **147**: 53–62.
- Vondrušková, E., van den Burg, J., Zíková, A., Ernst, N.L., Stuart, K., Benne, R., and Lukeš, J. (2005) RNA interference analyses suggest a transcript-specific regulatory role for mitochondrial RNA-binding proteins MRP1 and MRP2 in RNA editing and other RNA processing in *Trypanosoma brucei*. *J Biol Chem* **280**: 2429–2438.
- Wiedemann, N., Urzica, E., Guiard, B., Muller, H., Lohaus, C., Meyer, H.E., *et al.* (2006) Essential role of Isd11 in mitochondrial iron-sulfur cluster synthesis on Isu scaffold proteins. *EMBO J* **25**: 184–195.
- Žárský, V., Tachezy, J., and Doležal, P. (2012) Tom40 is likely common to all mitochondria. *Curr Biol* **22**: R479–R481.
- Zheng, L.M., White, R.H., Cash, V.L., Jack, R.F., and Dean, D.R. (1993) Cysteine desulfurase activity indicates a role for Nifs in metallocluster biosynthesis. *Proc Natl Acad Sci USA* **90**: 2754–2758.

Supporting information

Additional supporting information may be found in the online version of this article at the publisher's web-site.